Biochemical Pharmacology 84 (2012) 1318–1331

Contents lists available at SciVerse ScienceDirect

Biochemical Pharmacology

journal homepage: www.elsevier.com/locate/biochempharm

PARP inhibition potentiates the cytotoxic activity of C-1305, a selective inhibitor of topoisomerase II, in human BRCA1-positive breast cancer cells☆

Józefa Węsierska-Gądek [a,*], Nora Zulehner [a], Franziska Ferk [b], Andrzej Składanowski [c], Oxana Komina [a], Margarita Maurer [a]

[a] Cell Cycle Regulation Group, Dept. of Medicine I, Div.: Institute of Cancer Research, Comprehensive Cancer Center, Medical University of Vienna, Borschkegasse 8a, A-1090 Vienna, Austria
[b] Umweltoxikologie, Dept. of Medicine I, Div.: Institute of Cancer Research, Comprehensive Cancer Center, Medical University of Vienna, Borschkegasse 8a, 1090 Vienna, Austria
[c] Dept. of Pharmaceutical Technology and Biochemistry, Gdańsk University of Technology, Narutowicza 11/12, 80-952 Gdańsk, Poland

ARTICLE INFO

Article history:
Received 30 May 2012
Accepted 25 July 2012
Available online 14 August 2012

Keywords:
DNA strand breaks
Caspase-3 activation
Apoptosis
Cell cycle
G_2 arrest
Potential of mitochondrial membrane

ABSTRACT

Two cellular proteins encoded by the breast and ovarian cancer type 1 susceptibility (*BRCA1* and *BRCA2*) tumor suppressor genes are essential for DNA integrity and the maintenance of genomic stability. Approximately 5–10% of breast and ovarian cancers result from inherited alterations or mutations in these genes.

Remarkably, *BRCA1/BRCA2*-deficient cells are hypersensitive to selective inhibition of poly(ADP-ribose)polymerase 1 (PARP-1), whose primary functions are related to DNA base excision repair; PARP-1 inhibition significantly potentiates the cytotoxicity of various anti-cancer drugs, including inhibitors of topoisomerase I and II.

In the present study, we examined the anti-proliferative and pro-apoptotic effects of C-1305, a selective inhibitor of topoisomerase II, on human breast cancer cell lines with different *BRCA1* and *p53* statuses. BRCA1-competent breast cancer cell lines exhibited different responses to topoisomerase II inhibition. BT-20 cells that express high levels of BRCA1 levels were most resistant to C-1305 than other tested cells. Surprisingly, pharmacological interference with PARP-1 activity strongly inhibited their proliferation and potentiated the efficacy of C-1305 treatment. In contrast, PARP-1 inhibition only weakly affected the proliferation of BRCA1-deficient SKBr-3 cells and was not synergistic with the effects of C-1305. Further experiments revealed that the inhibition of PARP-1 in BT-20 cells caused the accumulation of DNA strand breaks and induced caspase-3 dependent apoptosis. These results seem to indicate that PARP-1 inhibition can potentiate the cytotoxicity of anti-cancer drugs in cancer cells with functional BRCA1 and suggest that mutations in other DNA repair proteins may render cancer cells more sensitive to interference with PARP-1 activity.

1. Introduction

Breast cancer is the most common malignancy in women and the second most prevalent cause of cancer-linked death in women (for reviews, see [1,2]). It is a conglomerate of diseases of the breast and arises from the misregulation of several essential cellular pathways (notably, those controlling cellular metabolism, cell cycle progression, cell proliferation, and apoptosis), with different variants having different signature characteristics and family histories (for reviews, see [3,4]). The identification of molecular signatures for different types of breast cancers over the last two decades has facilitated the development of targeted therapeutic strategies (for a review, see [5]).

Individuals with first-degree relatives having germline mutations in genes such as breast and ovarian cancer type 1 or 2 susceptibility (*BRCA1* or *BRCA2*) genes are subject to an increased risk of developing breast cancer [6]. Approximately 5–10% of breast and ovarian cancers result from inherited alterations or mutations in these genes. The BRCA1 and BRCA2 proteins are both involved in repairing double stranded DNA breaks by homologous recombination (HR), a process that is essential for DNA integrity and the maintenance of genomic stability [7–9].

☆ *Grant sponsor*: The work was partially supported by a grant from the Austrian Funding Agency FWF (grant no. P19894-B11) and by a grant from Center for International Cooperation & Mobility WTZ (no. PL 06/2012).

Abbreviations: BER, base excision repair; BRCA1, breast cancer type 1 susceptibility protein; HMC, Hoffman modulation contrast; HR, homologous recombination; NER, nucleotide excision repair; NHEJ, non-homologous end joining; MMP, mitochondrial membrane potential; PARP-1, poly(ADP-ribose)polymerase-1; PD, Petri dish; PVDF, polyvinylidene difluoride; TOPO, topoisomerase; WCL, whole cell lysate; WT, wild-type.

* Corresponding author. Tel.: +43 1 40160 57592; fax: +43 1 40 60 957592.
E-mail address: Jozefa.Gadek-Wesierski@meduniwien.ac.at (J. Węsierska-Gądek).

0006-2952 © 2012 Elsevier Inc. Open access under CC BY-NC-ND license.
http://dx.doi.org/10.1016/j.bcp.2012.07.024

In this context it is important to note that most conventional anti-cancer drugs such as alkylating agents, cross-linking agents, and topoisomerase inhibitors affect the integrity of DNA either directly or indirectly, resulting in the formation of single or double stranded breaks (for reviews, see: [10]). If these breaks are not repaired, the resulting persistent DNA damage can give rise to mutations and genomic instability that subsequently cause secondary cancers [11–13] or cell death [14], with the precise outcome depending on the overall extent of breakage. Interestingly, it has been found that DNA-repair deficient cancer cells (such as those with *BRCA 1/2* mutations) are more sensitive to inhibitors of poly(ADP-ribose)polymerase 1 (PARP-1), whose primary functions are related to DNA base excision repair (BER) [15–19]. Based on this observation, a new therapeutic approach termed "synthetic lethality" has been developed that relies on the conditional blockage of BER in DNA-repair deficient cancer cells [20]. Treatment with selective inhibitors of PARP-1 (a nuclear enzyme involved in the signaling of DNA damage and BER) in conjunction with radiation or cytotoxic anti-cancer agents such as topoisomerase (TOPO) type I or II inhibitors can induce severe genomic instability that leads to cell death. In recent years, the synergistic benefit of combining PARP-1 inhibition with anti-cancer drug treatment has been demonstrated in several pre-clinical models, and multiple PARP-1 inhibitors for use in treatments of this kind have been developed.

This paper describes an investigation into the sensitivity of breast cancer cells to C-1305, a selective inhibitor of TOPO II. A range of cells that differed in terms of the functional status of *BRCA1* and *p53* were considered. Different BRCA1-competent breast cancer cell lines exhibited different responses to C-1305. BT-20 cells expressing high levels of BRCA1 were most resistant to C-1305. However, pharmacological inhibition of PARP-1 activity strongly inhibited their proliferation and potentiated the efficacy of C-1305 treatment. In contrast, PARP-1 inhibition had only modest effects on the proliferation of BRCA-1-deficient SKBr-3 cells. These unexpected results indicate that interference with BER can potentiate the cytotoxicity of anti-cancer drugs in cancer cells with functional BRCA1 and suggest that mutations in other DNA repair proteins render cancer cells sensitive to inhibition of PARP-1 activity.

2. Material and methods

2.1. Drugs and chemicals

The triazoloacridone compound C-1305 used in this work was synthesized at the Department of Pharmaceutical Technology and Biochemistry (Gdańsk University of Technology) by Dr. Barbara Horowska. A stock solution of triazoloacridone (base-free) was prepared in 0.2% lactic acid. NU1025, an inhibitor of PARP-1 from AXON Medchem BV (Groningen, Netherlands) and camptothecin CPT), a quinoline alkaloid which inhibits topoisomerase I, from Calbiochem-Novabiochem Corporation (La Jolla, CA), were stored as a stock solution in DMSO. All drugs were stored at −20 °C until use.

2.2. Cells and treatment

Human primary breast cancer cell lines were purchased from the American Type Culture Collection (ATCC, Manassas, VA). The following cell lines were used: human MCF-7, BT-20 [21], and SKBr-3 [22] breast carcinoma cells. MCF-7 cells were grown as a monolayer in phenol red-free Dulbecco's medium supplemented with 10% fetal calf serum (FCS) at 37 °C under an atmosphere containing 8% CO_2 [23]. SKBr-3 cells were cultivated in DMEM medium with 10% FCS, and BT-20 cells in RPMI with 10% FCS. Twenty-four hours after plating (at 60–70% confluence), the cells were treated with the triazoloacridone compound C-1305 at concentrations ranging from 1 to 10 μM, and with NU1025 at a final concentration of 100 or 200 μM. The two drugs were applied separately or simultaneously, for the periods of time indicated in Figs. 2–10.

2.3. Antibodies

The following specific primary antibodies were used to detect the relevant proteins: mouse monoclonal anti-p53 antibody DO-1 and rabbit polyclonal anti-H2AX antibody (from BioLegend, San Diego, CA), anti-BRCA-1 rabbit polyclonal antibody (from Upstate Cell Signaling Solutions, Lake Placid, NY), anti-ER-α rabbit polyclonal antibody (from Sigma–Aldrich, St. Louis, MO), anti-phospho-histone H2AX (Ser139) rabbit polyclonal antibody (from Cell Signaling Technology Inc., Danvers, MA), anti-DBC-1 mouse monoclonal antibody (from Abcam plc, Cambridge, UK), and mouse monoclonal anti-actin antibody (clone C4, ICN Biochemicals, Aurora, OH). Appropriate secondary antibodies linked to horseradish peroxidase (HRP) were obtained from R&D Systems (Minneapolis, MN).

2.4. Detection of chromatin changes in individual cells by fluorescence microscopy

Cells grown in 35 mm Petri dishes were treated with C-1305, NU1025 or a combination of the two for the indicated lengths of time and then washed three times in PBS. The washed cells were immediately fixed in 3.7% paraformaldehyde in PBS, then washed 4 times in PBS and stained with Hoechst 33258 dissolved in PBS at a final concentration of 1.5 μg/ml [24]. The stained cells were inspected under a fluorescence microscope (Eclipse TE300 inverted microscope, Nikon Corporation, Tokyo).

2.5. Determination of numbers of living cells

The numbers of viable human breast cancer cells and their sensitivities to the tested drugs at various concentrations were determined using CellTiter-Glo™ assays (Promega Corporation, Madison, WI). As described previously [25], the CellTiter-Glo™ luminescent cell viability assay measures luminescent signals, which are correlated with cellular ATP levels. Tests were performed at least in quadruplicate, and the cells' luminescence was measured using a Wallac 1420 Victor multilabel, multitask plate counter (Wallac Oy, Turku, Finland). Each data point represents the mean ± SD (bars) of replicates from at least three independent experiments (Figs. 2–4). The effects of the combined C-1305 and NU1025 treatments are shown in Fig. 4.

2.6. Quantitative analysis of the mitochondrial membrane potential by flow cytometry

Mitochondrial depolarization was monitored using the cationic carbocyanine dye JC-1 (Molecular Probes Inc., Eugene, OR) as previously described [26]. Control and drug-treated cells were harvested, washed and incubated with the dye at a final concentration of 10 μM for 5 min followed by extensive washings in PBS and immediate two-color analysis by flow cytometry. JC-1 accumulates in the mitochondria of intact cells if the mitochondrial membrane potential is within the normal range, forming fluorescent red aggregates known as J-aggregates that emit at 570 nm in response to excitation at 488 nm. Mitochondrial depolarization in apoptotic cells causes the aggregates to dissociate into green fluorescent monomers

emitting at 530 m in response to excitation at 488 and 530 nm.

2.7. Determination of the activity of caspase-3/7

The activity of caspase-3/7 was determined using the Caspase-3-GLO Assay (Promega Corporation, Madison, WI) with a luminogenic caspase-3/7 substrate harboring the caspase-3/7 DEVD sequence as described previously [24,27]. Human BT-20 breast cancer cells were plated into 96-well microtiter plates. Twenty-four hours after plating, the cells were treated with C-1305, NU1025 or a combination of the two as listed in Fig. 9. As a positive control, BT-20 cells treated for 72 h with CPT at a final concentration of 0.2 and 2 μM were used. After termination of the treatment, equal volumes of the Caspase-3-GLO reagent were added and the probes were incubated at 37 °C for different periods of time to identify the best signal-to-background ratio. The generated luminescence was measured at intervals of 30 min. The luminescence, which is directly proportional to the amount of activated caspase-3/7, was measured using a Wallac 1420 Victor multifunction plate reader (Wallac Oy, Turku, Finland). The measured caspase-3/7 activity was normalized against the number of living cells as determined by the CellTiter-Glo™ assay and expressed as a percentage of the control value. Each data point represents the mean ± SD (bars) of two independent experiments, each of which was performed in quadruplicate or more.

2.8. Measurement of DNA concentration in single cells by flow cytometry

The DNA contents of single cells were measured by flow cytometry using the method of Vindelov [28], with slight modifications as described elsewhere [27]. Briefly, the adherent cells were detached from the substratum by limited trypsinization and then all cells were harvested by centrifugation and washed in PBS. Aliquots of 1×10^6 cells were stained with propidium iodide as previously described and their fluorescence was measured using a Becton Dickinson FACScan flow cytometer (Becton Dickinson, Franklin Lakes, NJ) after at least 2 h incubation at +4 °C in the dark. The cellular DNA concentration was evaluated using ModFIT LT™ cell cycle analysis software (Verity Software House, Topsham, ME) and DNA histograms were generated using the CellQuest™ software package (Becton Dickinson, Franklin Lakes, NJ).

2.9. Single-cell gel electrophoresis (SCGE)

The formation of DNA strand breaks was assessed by the single cell gel electrophoresis (SCGE) assay performed under alkaline conditions. The terms "SSGE" or "Comet" are used interchangeably throughout this report. The experiments were carried out according to the international SCGE guidelines [29,30] as described previously [24]. The cells investigated were human BT-20 breast cancer cells and cells that had been exposed for 24 h to C-1305 at final concentrations of 2 μM and 5 μM, to NU1025 at a final concentration of 100 μM alone, or to some combinations of the two drugs. Cells were analyzed immediately after termination of treatment and also after being washed out and subjected to an additional 48 h' post-incubation in a drug-free medium or in media containing 100 μM NU1025. The cells were harvested in PBS and their viability was determined using the Trypan blue exclusion test [31]. In all cultures, the cells' vitality was ≥80%. Three cultures were prepared in parallel for each experimental point considered, and for each treatment 150 cells were analyzed for Comet formation. To monitor DNA migration, cell suspensions (1×10^5 cells) were mixed with low melting point agarose (0.5% LMA) and transferred to agarose-coated slides (1.5% NMA). The slides were then immersed in a lysis solution (1% Triton X-100, 10% DMSO, 2.5 M NaCl, 100 mM EDTA, 10 mM Trizma base). After lysis (pH 10.0) and electrophoresis (30 min, 300 mA, 1.0 V/1 cm corresponding to 25 V, at 4 °C, pH > 13), the gels were stained with ethidium bromide (20 μg/ml). The resulting slides were examined under a fluorescence microscope (Nikon EFD-3, Tokyo, Japan) using 25-fold magnification. DNA migration was determined based on tail intensity (% DNA in tail) using a computer-aided Comet assay image analysis system (Comet Assay IV, Perceptive Instruments, UK).

2.10. Electrophoretic separation of proteins and immunoblotting

Total cellular proteins dissolved in SDS sample buffer were separated on 10%, 12% or 15% SDS slab gels, transferred electrophoretically onto polyvinylidene difluoride membrane (PVDF) (GE Healthcare UK Ltd, Little Chalfont, Buckinghamshire, England (formerly Amersham Biosciences) and immunoblotted as previously described [32,33]. Equal protein loading was confirmed by Ponceau S staining. To determine the phosphorylation status of selected proteins, antibodies recognizing site-specific phosphorylated proteins were diluted to a final concentration of 1:1000 in 1% BSA in Tris–saline–Tween-20 (TST) buffer [24]. In some cases, blots were used for sequential incubations. Immune complexes were detected after incubation with appropriate HRP-coupled secondary antibodies using chemiluminescent ECL Plus™ Western Blotting Reagents from GE Healthcare. Chemiluminescence was detected after exposing the blots to film or by analysis using ChemiSmart5100 apparatus (PEQLAB, Biotechnologie GmbH, Erlangen, Germany).

2.11. Analysis of interactions using the CalcuSyn method

Two methods of interaction analysis were used to determine whether the drug combination exhibited synergistic, additive, or antagonistic effects. The first was the combination index (CI) method of Chou and Talalay [34]. The CalcuSyn software package (Version 2.0, Biosoft, Cambridge, UK), which is based on this method and takes into account both potency [median dose (D_m) or IC_{50}] and the shape of the dose-effect curve (the m value), was used to calculate the combination index (CI). The program automatically graphs its output and produces reports of summary statistics for all of the drugs considered, together with a detailed analysis of drug interactions including the combination index (CI). A combination is considered to be synergistic if CI <1, additive if CI = 1, and antagonistic if CI > 1. For this analysis, data were obtained on the effects of the combined C-1305 and NU1025 treatments at each tested concentration. The fraction of cells affected and the corresponding combination index values were calculated for each concentration.

2.12. Statistical analyses

Statistical analyses were performed using GraphPad Prism software (GraphPad Software, Inc., La Jolla, CA) and significance levels were evaluated using Bonferroni's and Dunnett's Multiple Comparison Tests. Differences between treatments were deemed to be extremely significant, very significant, significant and not significant if their p values (according to Bonferroni's comparison test) were <0.001, <0.01, 0.01 < p < 0.05 and >0.05, respectively. In the tables and figures such differences are indicated by three asterisks (***), two asterisks (**), one asterisk (*) and no asterisk, respectively.

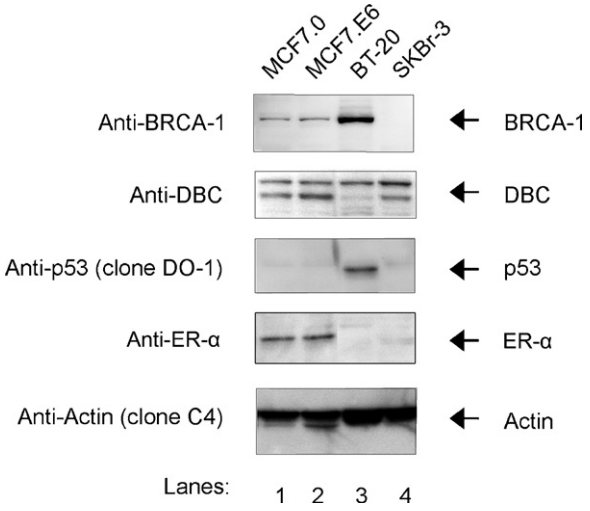

Fig. 1. Differential signature of human breast cancer cells examined in this study. WCLs prepared from four breast cancer cell lines were analyzed by immunoblotting after separation on 10% SDS slab gels. Blots were incubated with antibodies directed against BRCA1, DBC-1, ER-α and p53. Immune complexes were detected after incubation with appropriate secondary antibodies linked to HRP and chemiluminescence reagent ECL Plus™ (GE Healthcare). Chemiluminescence was monitored using ChemiSmart5100 apparatus (PEQLAB, Biotechnologie GmbH, Erlangen, Germany). Equal protein loading was confirmed by Ponceau S staining of membranes and incubation with anti-actin antibodies. BT-20, SKBr-3 cells and two cell MCF-7 derived cell clones (MCF-7.0 cells transfected with empty CMV vector and MCF-7.E6 transfected with CMV vector expressing HPV-encoded E6 oncoprotein) were loaded.

3. Results

3.1. Differential signature of human breast cancer cells examined in this study

We initially used immunoblotting to analyze cellular levels of proteins that are known to be characteristic of the breast cancer cell lines examined in this work. In keeping with previous reports, BRCA1 was not detected in SKBr-3 cells [22]. Conversely, BRCA1 was strongly expressed in human BT-20 cells, to an appreciably greater extent than was observed for MCF-7 cells (Fig. 1). The dual-acting protein DBC-1 (Deleted in Breast Cancer-1) was expressed at similar levels in all analyzed cell lines, and p53 protein was detected in both ER-α negative cancer cell lines (BT-20 and SKBr-3; to an appreciably greater extent in BT-20 cells). As expected, the p53 protein was not present at detectable levels in unstressed control MCF-7 cells that harbor the wt *TP53* gene (Fig. 1).

3.2. Pharmacological interference with PARP-1 activity strongly inhibits proliferation of BT-20 cells with strong expression of BRCA1

Based on previous results, it might have been expected that of the cell lines tested, those deficient in BRCA1 expression would be most sensitive to PARP-1 inhibition. Surprisingly however, the cell line that was most strongly affected by pharmacological interference with PARP-1 activity was that with the highest BRCA1 levels – the BT-20 line (Fig. 2). The anti-proliferative action of the PARP-1 inhibitor was both concentration- and time-dependent, but continuous treatment for 48 h caused very statistically significant reductions in the number of living BT-20 cells even at the lower NU1025 dose (C_E = 100 μM) (Fig. 2). In contrast, the proliferation of BRCA1-deficient SKBr-3 cells was almost completely unchanged after 48 h' exposure to the PARP-1 inhibitor (Fig. 2).

3.3. BRCA1-deficient SKBr-3 cells are most sensitive to the inhibition of topoisomerase II by C-1305

In the second phase of the investigation, we determined the sensitivity of the breast cancer cells to C-1305, a selective inhibitor of topoisomerase II. Of the tested cancer cells, it was the BRCA1-deficient SKBR-3 line whose proliferation was most strongly inhibited by C-1305 (Fig. 3), whereas human BT-20 breast cancer cells (which have the highest BRCA1 levels of the tested lines) were most resistant to treatment with C-1305. Treatment with 10 μM C-1305 for 24 h reduced the number of living BT-20 cells by approximately 15% whereas the same treatment reduced the number of living SKBr-3 cells by almost 60%. As previously reported, C-1305 has a long-lasting effect [24]. After 24 h' exposure to C-1305, the treated cells were washed and incubated for 48 h on drug-free media. Further reductions in the number of living cells were observed during this post-incubation period (Fig. 3), with the number of living BT-20 cells falling by approximately 40%. The number of living cells from the MCF-7 and SKBr-3 lines fell by almost 85 and 95%, respectively. These results clearly show that the proliferation of human SKBr-3 cells was most strongly affected by treatment with C-1305.

3.4. Inhibition of PARP-1 potentiates the efficacy of C-1305 treatment exclusively in BT-20 cells

Because human SKBr-3 cells were insensitive to PARP-1 inhibition, our subsequent experiments examining the interaction between PARP-1 inhibition and TOPO-II inhibition focused exclusively on the human MCF-7 and BT-20 breast cancer lines. Concurrent inhibition of PARP-1 activity in human MCF-7 cells

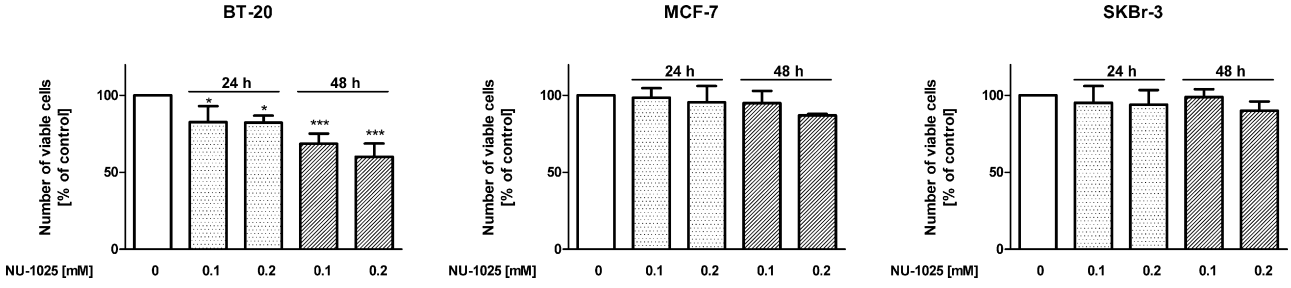

Fig. 2. Pharmacological interference with PARP-1 activity strongly inhibits proliferation of BT-20 cells with strong expression BRCA1. Exponentially growing breast cancer cells (BT-20, MCF-7 and SKBr-3) were plated in 96-well microtiter plates and 24 h after plating were treated with NU1025 at indicated concentrations for 24 h or 48 h. The numbers of viable cells were determined directly after the treatment using CellTiter-Glo™ assays (Promega Corporation, Madison, WI). The data represent mean values from at least three independent experiments, each performed in quadruplicate. Results were analyzed using GraphPadPrism software (GraphPad Software, Inc.). The statistical significance of the observed reductions in cell numbers following treatment were calculated using Dunnett's Multiple Comparison test. PARP-1 inhibitor reduced significantly (24 h) and very significantly (after 48 h) the numbers of viable BT-20 cells. Asterisks located directly above individual bars denote statistically significant differences between the corresponding treatment and the control. Single asterisks denote significant differences at the $p < 0.05$ level. Triple asterisks denote significant differences at the $p < 0.001$ level.

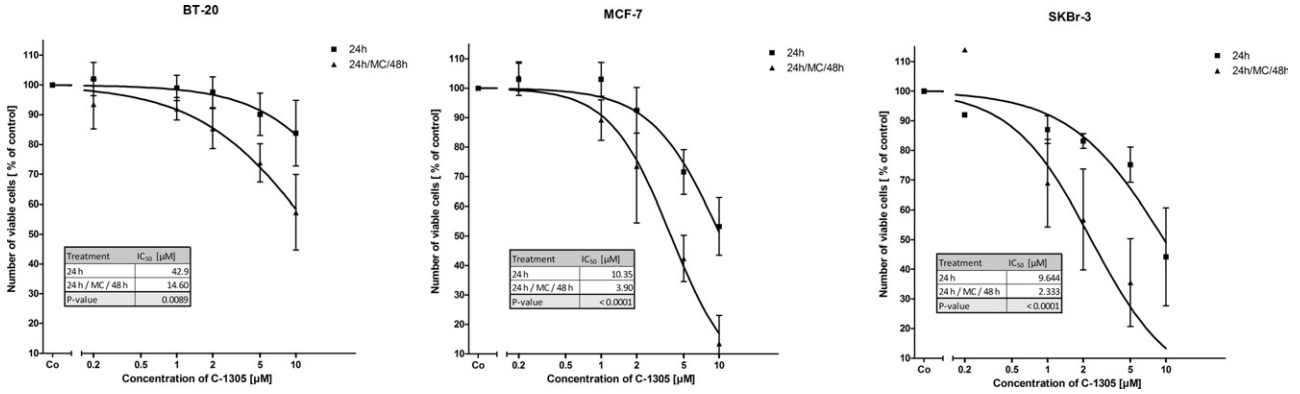

Fig. 3. BRCA1-deficient SKBr-3 cells are most sensitive to the inhibition of topoisomerase II by C-1305. Exponentially growing human breast cancer cells (BT-20, MCF-7 and SKBr-3) were plated in 96-well microtiter plates and 24 h after plating were treated with C-1305 at indicated concentrations for 24 h. The numbers of viable cells were determined directly after the treatment, or alternatively medium was changed and cells were post-incubated in a drug-free medium for 48 h using CellTiter-Glo™ assays (Promega Corporation, Madison, WI). The data were analyzed as described in detail in Fig. 2. Dose–response curves were calculated by nonlinear regression analyses. IC_{50} values determined from dose–response curves are shown.

caused only a slight increase in the anti-proliferative effect of C-1305 after 24 h (Fig. 4A, left panel). Similarly, pharmacological inactivation of PARP-1 during the post-incubation of C-1305-treated MCF-7 cells did not greatly increase the effect of the TOPO II inhibitor (Fig. 4A, right panel). Notably, changing of the sequence of drug administration by first treating the cells with NU1025 for 24 h, washing, then treating with C-1305 + NU1025 for 48 h (Fig. 4A, right panel) alleviated the anti-proliferative effect of the TOPO II inhibitor.

In contrast, NU1025 strongly enhanced the cytotoxic effects of C-1305 on human BT-20 cells (Fig. 4B). Concurrent inhibition of PARP-1 activity enhanced the cytotoxic effects of C-1305 after 24 h; this effect was statistically significant and was more pronounced at the higher C-1305 concentration (C_E = 5 μM)

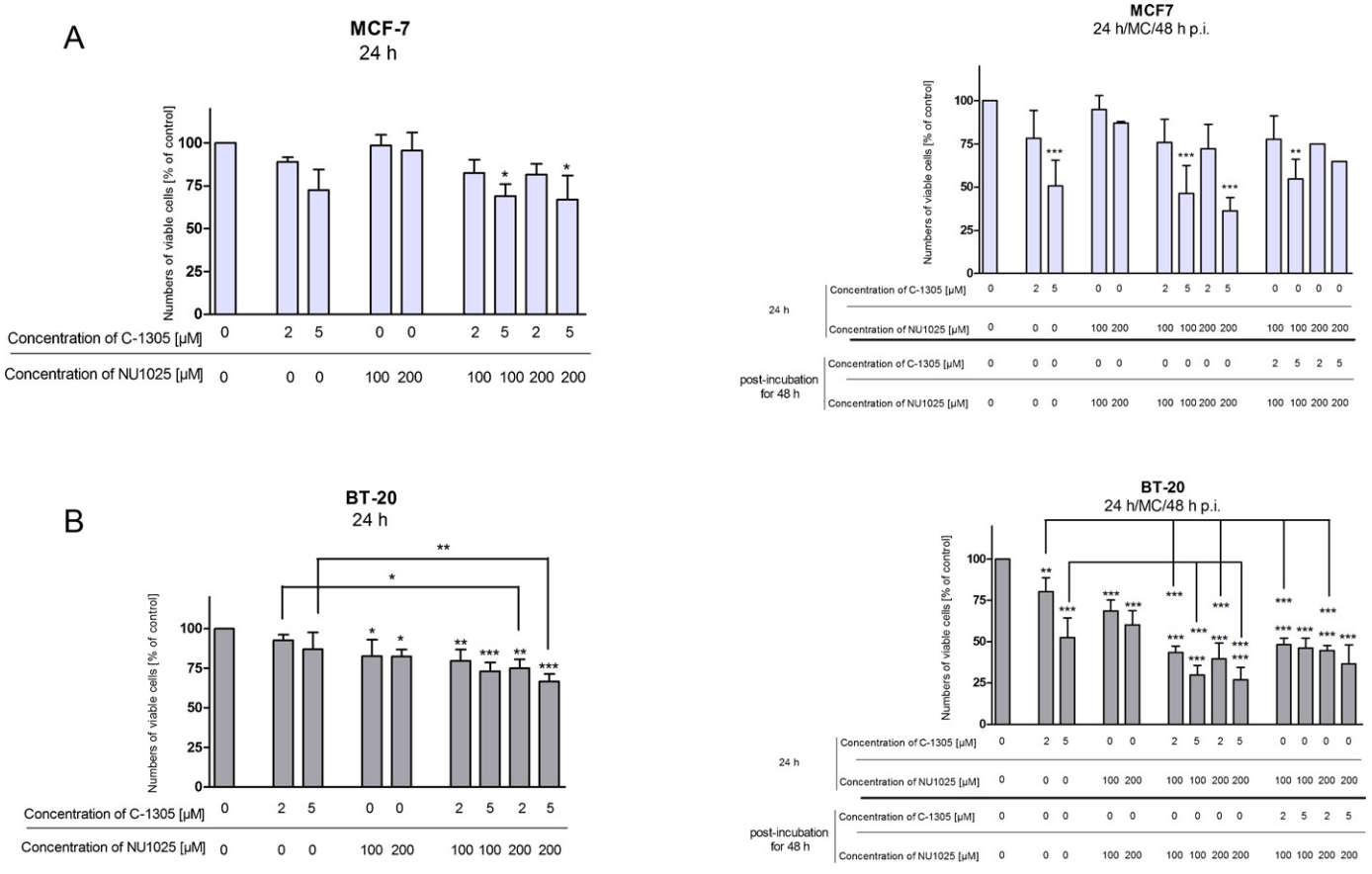

Fig. 4. Inhibition of PARP-1 potentiates the efficacy of C-1305 treatment exclusively in BT-20 cells. Human MCF-7 and BT-20 breast cancer cells were plated as described in Fig. 2. Cells were treated with C-1305 and NU1025, or their combination at indicated concentrations. The data were analyzed as described in detail in Fig. 2. The statistical significance of the observed reductions in cell numbers following treatment was calculated using Dunnett's and Bonferroni's Multiple Comparison test. Asterisks located directly above individual bars denote statistically significant differences between the corresponding treatment and the control. Asterisks located directly at the end of a line connecting two bars denote statistically significant differences between the indicated treatments. Single asterisks denote significant differences at the $p < 0.05$ level. Double asterisks denote significant differences at the $p < 0.01$ level. Triple asterisks denote significant differences at the $p < 0.001$ level.

(Fig. 4B; left panel). C-1305 has long-lasting effects; these results demonstrate that PARP-1 inhibition with NU1025 can potentiate the effects of C-1305 even if the former is applied some time later than the latter. Inactivation of PARP-1 during co-treatment with C-1305 for 24 h and during the subsequent 48-h post-incubation doubled the cytotoxic effect of the TOPO II inhibitor (Fig. 4B; right panel). All of these effects were statistically significant. Notably, increasing the dosage of the PARP-1 inhibitor did not enhance the cytotoxicity of C-1305.

3.5. The interaction between C-1305 and PARP-1 inhibition in BT-20 cells is strongly synergistic

Our discovery that treating BT-20 cells with a PARP-1 inhibitor potentiates the anti-proliferative action of C-1305 prompted us to investigate the interactions between two compounds using the CalcuSyn software package. The calculated combination index (CI) was less than 1 for all compound combinations tested, indicating a synergistic interaction between NU1025 (C_E = 100 and 200 μM) and C-1305 at concentrations ranging from 2 to 5 μM (Table 1). The interaction was additive (CI ± 1.011) when BT-20 cells were treated with 100 μM NU1025 for 24 h and then NU1025 was combined with 5 μM C-1305 during the 48 h post-incubation period. In contrast, the interaction between the two tested inhibitors in MCF-7 cells was additive after treatment for 24 h and CI increased to more than 1.2 after the post-incubation, indicating an antagonistic relationship.

3.6. Interfering with PARP-1 activity has different effects on cell cycle progression in BT-20 and MCF-7 cells

To determine how NU1025 modulates cell cycle progression in human BT-20 and MCF-7 breast cancer cells, exponentially growing cells were exposed to NU1025 for 24 h at final concentrations of 100 and 200 μM. The cells were then harvested and the DNA concentration of single cells was determined by flow cytometric measurement of their fluorescence intensity following propidium iodide staining. In exponentially growing MCF-7 cells, treatment with the PARP-1 inhibitor for 24 h increased the abundance of S-phase cells by approximately 10% at the expense of the G_1 cell population (Fig. 5). However, extending the treatment for a longer period of time (24 h/MC/p.i. 48 h) yielded a distribution across the phases of the cell cycle similar to that observed for the untreated controls. In contrast, the number of S-phase cells decreased slightly when BT-20 cells were treated with NU1025 for 24 h or for 72 h overall (24 h/MC/p.i. 48 h); this was accompanied by a modest increase in the proportion of G_2-phase cells. These results indicate that by itself, pharmacological interference with PARP-1 activity has weak but opposed effects on cell cycle progression in the two human breast cancer lines considered in this work.

3.7. Inhibition of TOPO II affects cell cycle progression in human breast cancer cells

The effect of C-1305 on the distribution of breast cancer cells across the phases of the cell cycle was dose-dependent. At the lower dose considered (2 μM), the TOPO II inhibitor caused a decrease in the abundance of S-phase cells in both lines, with a corresponding increase in the proportion of G_1-phase cells (Fig. 5). These changes were transient; after washing out and post-incubation for 48 h in drug-free media, the distribution of cells across the phases of the cell cycle was similar to that in untreated control cells. However, at the higher dose (5 μM), C-1305 induced arrest at the G_2/M transition (Fig. 5). C-1305-induced G_2 arrest was more pronounced in MCF-7 cells (in which it caused an approximately threefold increase in the abundance of G_2 cells, from 15% to 40%) than in BT-20 (18% to 33%), and persisted in both cell lines after 48 h' post-incubation in a drug-free medium.

3.8. Impact of concurrent inactivation of PARP-1 and TOPO II on cell cycle progression

The observed changes in cell cycle distribution became more pronounced when C-1305 was applied in conjunction with NU1025 provided that both compounds were applied at the higher doses (5 μM C-1305 + 200 μM NU1025). In human MCF-7 cells, this combination caused a pronounced reduction in the proportion of S-phase cells after 24 h, with a corresponding increase in the abundance of G_1-phase cells. In contrast, treatment of BT-20 cells for 24 h with 5 μM C-1305 in conjunction with 200 μM NU1025 increased the proportion of S-phase cells and decreased that of G_1-phase cells. Taken together, these results show that inactivation of PARP-1 has very little or no impact on cell cycle progression and that the combination of the PARP-1 inhibitor with C-1305 has no significant impact on cell cycle progression in BT-20 cells.

3.9. Chromatin changes after inhibition of TOPO II and PARP-1 in breast cancer cells

We used *in situ* monitoring techniques to observe the changes in cell density and chromatin structure following the inhibition of

Table 1
Synergistic interaction between C-1305 and NU1025 in BT-20 cells.

24 h	100 μM NU1025		200 μM NU1025	
	2 μM C-1305	5 μM C-1305	2 μM C-1305	5 μM C-1305
BT-20	0.188	0.126	0.271	0.176
MCF-7	0.842	0.99	0.996	1.045
24 h	100 μM NU1025+		200 μM NU1025+	
	2 μM C-1305	5 μM C-1305	2 μM C-1305	5 μM C-1305
Post-incubation for 48 h	100 μM NU1025		200 μM NU1025	
BT-20	0.449	0.555	0.485	0.532
MCF-7	1.212	1.01	1.325	0.847
24 h	100 μM NU1025		200 μM NU1025	
Post-incubation for 48 h	100 μM NU1025+		200 μM NU1025+	
	2 μM C-1305	5 μM C-1305	2 μM C-1305	5 μM C-1305
BT-20	0.544	1.011	0.623	0.796
MCF-7	1.296	1.284	1.46	1.966

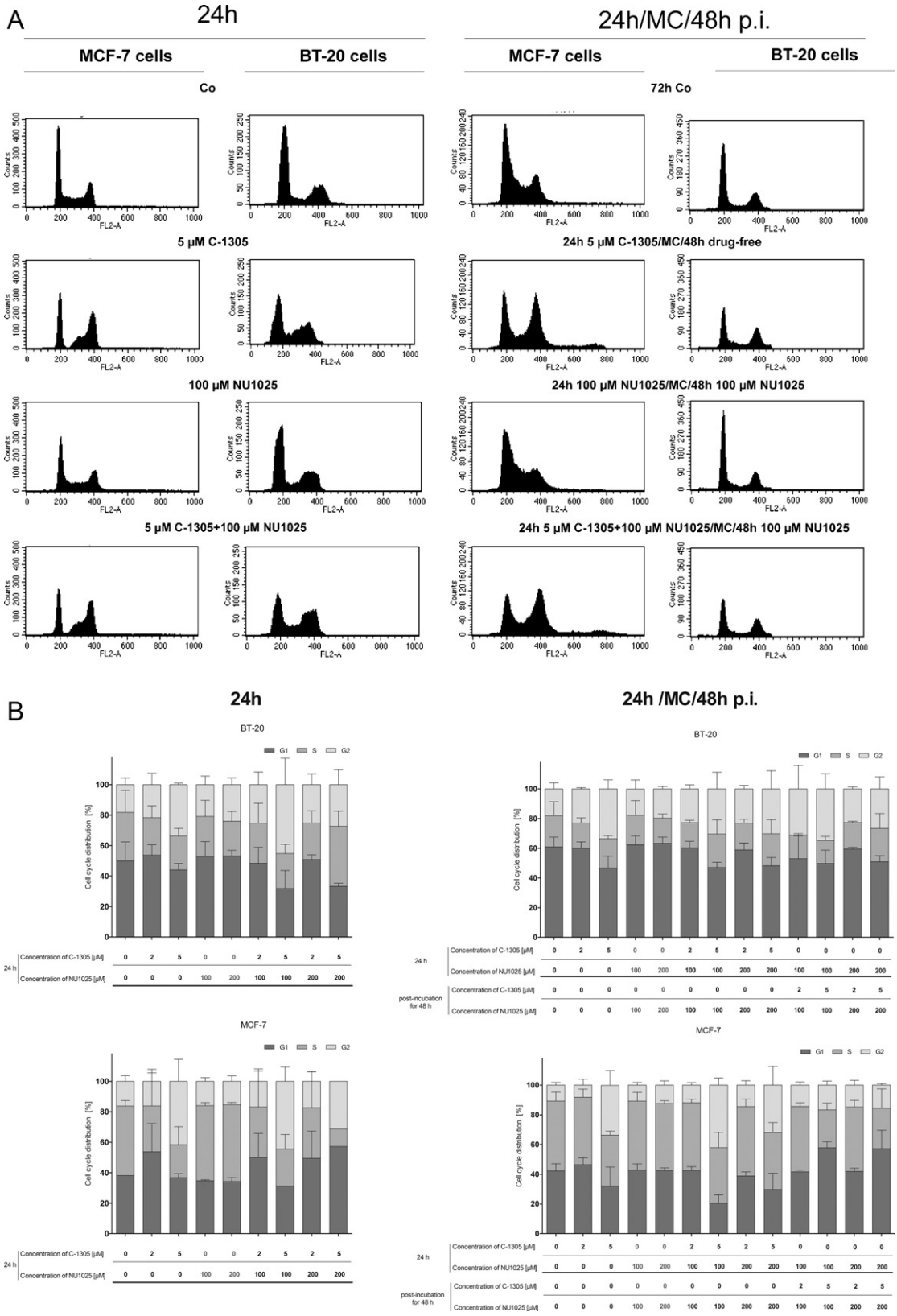

Fig. 5. Interference with TOPO II activity affects differentially the progression of cell cycle in BT-20 and MCF-7 cells. Exponentially growing human BT-20 and MCF-7 breast cancer cells were treated with C-1305, NU1025 or their combination at indicated concentrations for 24 h. Cells were harvested immediately after treatment or alternatively medium was changed and cells were post-incubated for 48 h. Harvested cells were stained with propidium iodide. DNA content in single cells was measured by flow cytometry. (A) DNA histograms obtained from a representative experiment were prepared using Cell Quest software. (B) Comparison of the inhibitors on the distribution of cells in specific cell cycle phases. DNA concentrations were evaluated using ModFIT software. The data represent mean values ± SD from three independent experiments.

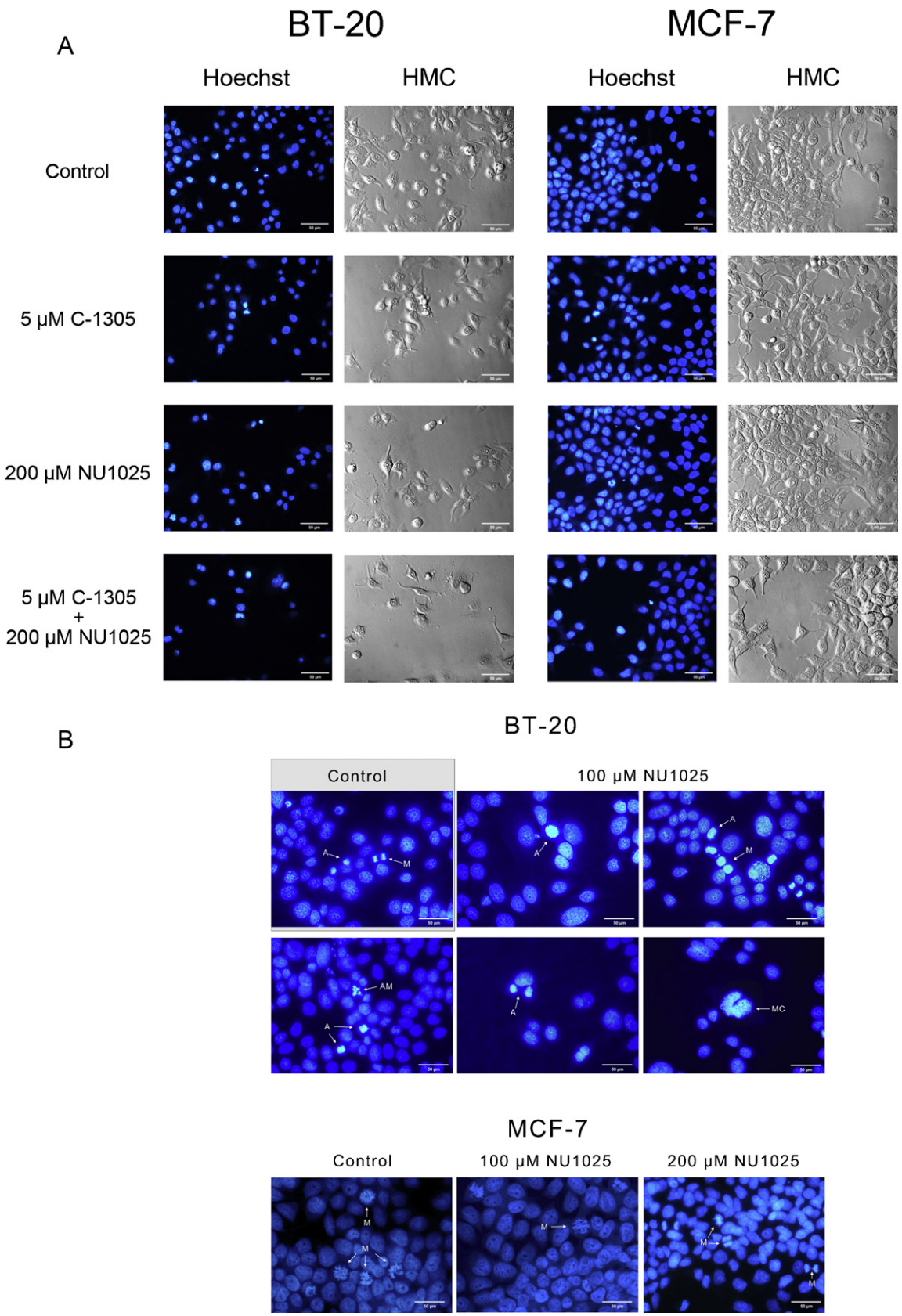

Fig. 6. Monitoring of changes in chromatin structure in breast cancer cells after inhibition of TOPO II and PARP-1. (A) Inhibition of PARP-1 strongly reduces the number of BT-20 cells but not of MCF-7 cells. Images taken at low magnification (10× objective). (B) Induction of apoptosis and mitotic catastrophe in BT-20 cells after inhibition of PARP-1. Images taken at higher magnification (60× objective). Untreated controls and cells treated with C-1305, NU1025 or their combination for 48 h were fixed and stained with Hoechst 33258. Cell density of monolayer, cell size and phenotype were inspected by light microscopy using Hoffman Modulation Contrast (HMC) and chromatin structure visualized by Hoechst 33258 staining was monitored by fluorescence microscopy. White bars represent 50 μm. A, apoptosis; AM, aberrant mitosis, M, mitosis; MC, mitotic catastrophe.

TOPO II and PARP-1 in breast cancer cells. Untreated control cells and cells exposed to either one inhibitor alone or both inhibitors in tandem were fixed and their chromatin was stained with Hoechst dye. Unlike MCF-7 cells, BT-20 cells were strongly affected by the inhibition of PARP-1 (Fig. 6A) and their density decreased substantially. Both mitotic cells and cells undergoing apoptosis were detected in the samples. Concurrent inhibition of PARP-1 and TOPO II caused a much more pronounced reduction in the number of living BT-20 cells. The proportion of apoptotic cells increased; a few dividing cells were also observed (Fig. 6B). Moreover, aberrant mitoses, mitotic catastrophe and apoptotic changes in mitotic cells were detected. These results indicate that inhibition of PARP-1 triggered apoptosis in BT-20 cells rather than stopping division.

3.10. PARP-1 inhibition causes DNA damage in BT-20 cells

Our next objective was to determine whether inhibiting PARP-1 with NU1025 would have any impact on DNA integrity. It is known that DNA damage induces site-specific phosphorylation of the H2AX protein *via* activation of stress kinases. We therefore used immunoblotting to quantitatively monitor changes in the phosphorylation status of this protein in breast cancer cells treated with inhibitors of PARP-1, TOPO II or both (Fig. 7). In MCF-7 cells, treatment with NU1025 did not cause increased phosphorylation of H2AX at Ser139 relative to the untreated control sample (Fig. 7). Surprisingly, PARP-1 inhibition strongly induced phosphorylation of H2AX in BT-20 cells. Furthermore, at the higher dose (C_E = 5 μM), C-1305 caused a pronounced increase in H2AX phosphorylation in MCF-7 cells but not in BT-20 cells. However, inhibition of PARP-1 in BT-20 cells in conjunction with C-1305 potentiated the phosphorylation of H2AX at Ser139. The changes in the phosphorylation status of the H2AX protein seem to reflect the sensitivity of both cancer cell lines to the treatment.

3.11. Inactivation of PARP-1 induces caspase-3-dependent apoptosis in BT-20 cells

Our next objective was to determine whether interfering with the activity of TOPO II and PARP-1 would promote pro-apoptotic changes in the studied breast cancer cells. To assess the impact of pharmacological inactivation of both enzymes on the mitochondrial membrane potential (MMP), we monitored the membrane potential using the electrochromic dye JC-1 [35]. JC-1 is a positively charged carbocyanine dye whose distribution between the subcellular compartments depends on the MMP. Untreated control MCF-7 and BT-20 cancer cells and cells treated with the inhibitors separately or together were detached from the substratum by limited trypsinization and then incubated with JC-1. After careful washing, the cells were immediately analyzed by flow cytometry. As shown in Fig. 8, the inhibition of TOPO II by C-1305 did not alter the membrane potential in BT-20 and MCF-7 cells, with fluorescent red J-aggregates being observed in both cases. After exposure to NU1025, the JC-1 aggregates disappeared from the mitochondria of several BT-20 cells and were replaced by the green fluorescent monomer, which accumulates in the cytosol. Concurrent inhibition of PARP-1 and TOPO II only caused strong disruption of the MMP when both inhibitors were used at the higher dose, but the observed changes were statistically significant. Decreases in the MMP are characteristic of apoptosis; they cause matrix condensation and redistribution of cytochrome c, thereby facilitating the

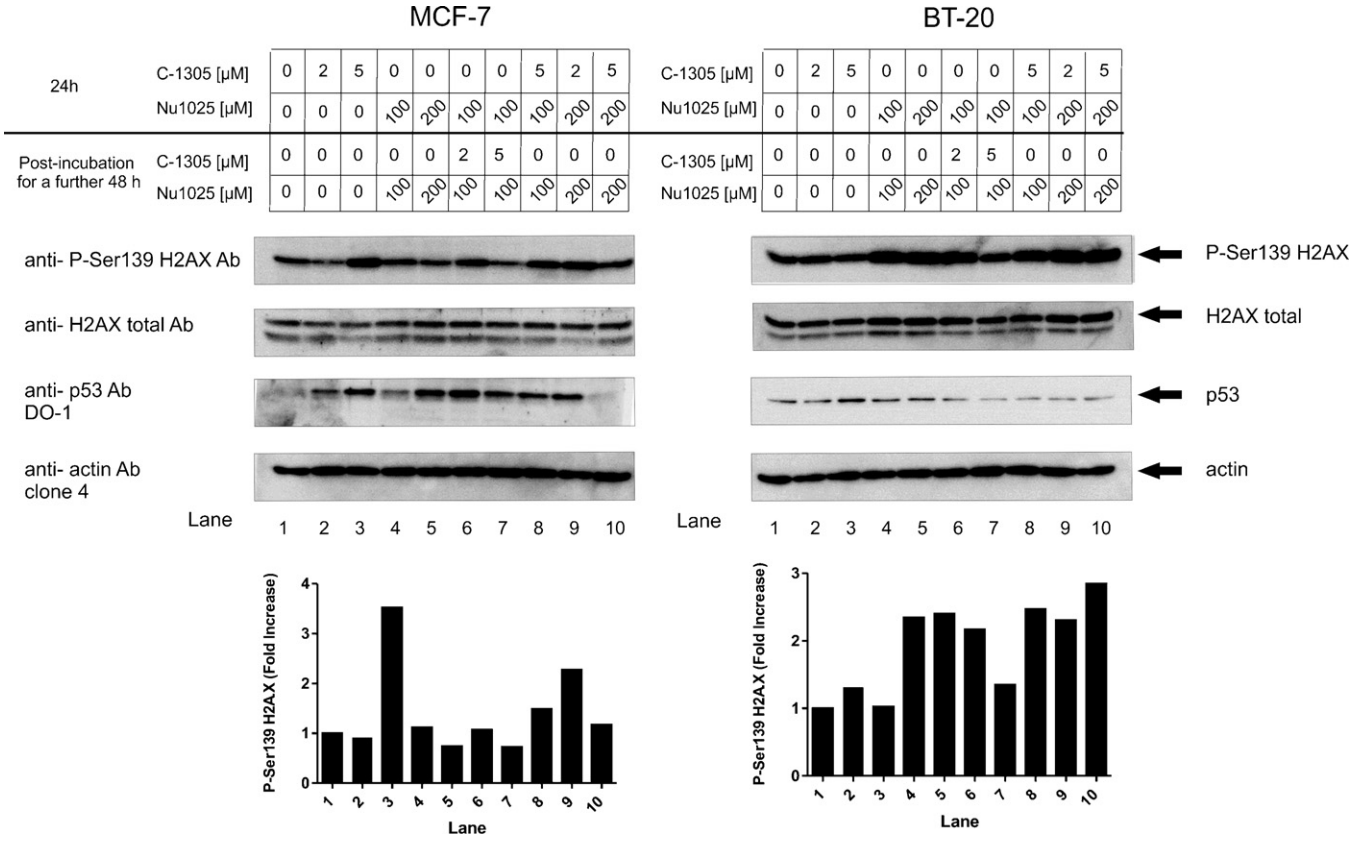

Fig. 7. PARP-1 inhibitor induces site-specific phosphorylation of H2AX and changes in p53 expression in human breast cancer cells. WCLs prepared from untreated control MCF-7 and BT-20 cells and cells exposed to either one inhibitor alone or both inhibitors in tandem were separated on SDS slab gels (10 or 15%) and analyzed by immunoblotting using indicated antibodies as described in detail in Fig. 1. The intensity of protein bands representing P-Ser139 H2AX and total H2AX protein in each lane was normalized against actin. Then P-Ser139 H2AX/H2AX ratio was calculated and normalized against the ratio calculated for the controls. The relative phosphorylation of H2AX was plotted in the diagram.

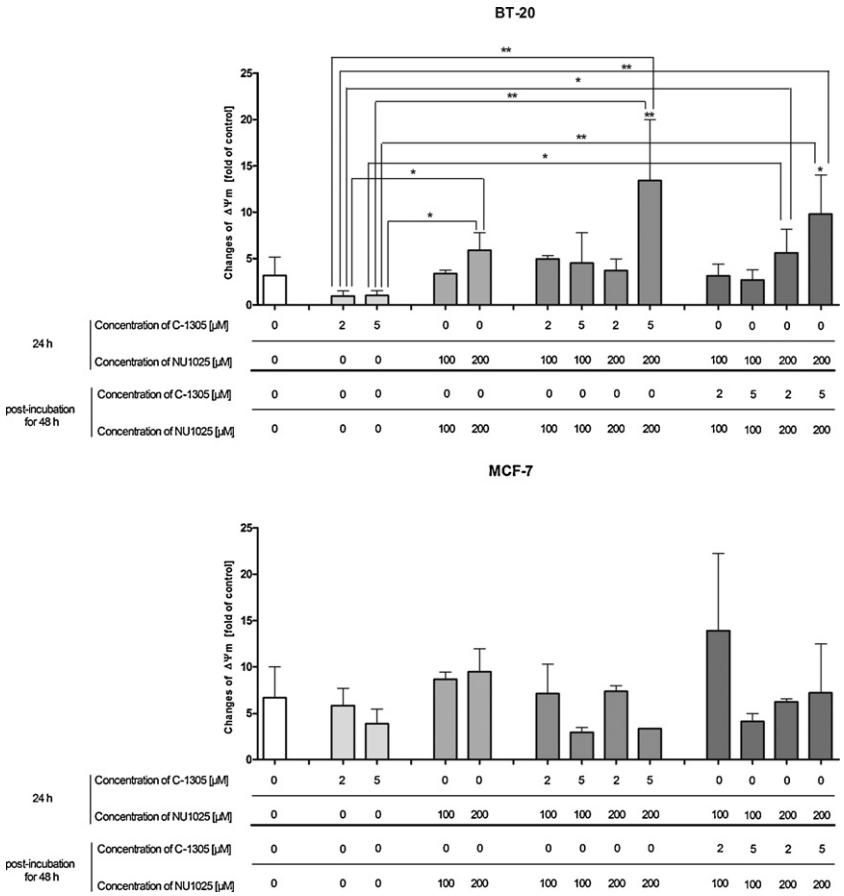

Fig. 8. Significant disruption of the MMP in human BT-20 breast cancer cells after concurrent inhibition of TOPO II and PARP-1. Exponentially growing human MCF-7 and BT-20 cells were treated with C-1305, NU1025 or their combination at indicated concentrations. After treatment cells were collected and incubated with JC-1 and directly after washing were analyzed by flow cytometry using the FITC channel for green monomers (Ex/Em = 510/527) and the PI channel for red-J-aggregates (Ex/Em = 585/590). The population of cells that lost the capability to aggregate JC-1 is shown in diagram. The statistical significance of the observed disruption of the MMP after treatment was calculated using Bonferroni's Multiple Comparison test. Asterisks located directly at the midpoint of a line connecting two bars denote statistically significant differences between the indicated treatments. Single asterisks denote significant differences at the $p < 0.05$ level. Double asterisks denote significant differences at the $p < 0.01$ level.

release of cytochrome c release and activation of the apoptotic cascade [36]. To determine the induction of downstream steps, the activity of effector caspases was measured in BT-20. While caspase 3/7 activity was not stimulated by inhibiting TOPO II (Fig. 9), it was strongly induced by PARP-1 inhibition. Simultaneous inhibition of PARP-1 and TOPO II also caused high caspase 3/7 activity, and the increase was statistically significant. Collectively, these results show that inhibition of PARP-1 potentiates a decrease in the MMP leading to an apoptotic cascade that strongly activates effector caspases.

3.12. Accumulation of DNA damage in BT-20 cells after inhibition of PARP-1 and TOPO II

Finally, to assess the DNA damaging activity of C-1305, we performed a single cell gel electrophoretic (SSGE) analysis. The level of DNA damage was quantified by determining the intensity of the DNA 'tail' according to updated international recommendations [29,30]. Human BT-20 cancer cells were treated with triazoloacridone and NU1025 alone or in tandem at the indicated final concentrations for 24 h. The cells were analyzed using the Comet assay immediately after treatment, or alternatively after a 48 h post-incubation in drug-free media or in media containing the PARP-1 inhibitor. Treatment with C-1305 for 24 h at a final concentration of 2 μM caused a low level of DNA damage in BT-20 cells; the observed increase in tail intensity was not statistically significant (Fig. 10). At a final C-1305 concentration of 5 μM, the level of DNA damage was somewhat higher. The cytotoxic effects of PARP-1 inhibition in BT-20 cells were much more pronounced; the Comets generated following NU1025 treatment had much greater tail intensities. Co-treatment with both C-1305 and the PARP-1 inhibitor caused a slight increase in the level of DNA damage, and the increase in DNA damage on going from TOPO-II inhibition (C-1305, C_E = 2 μM) alone to inhibition of both TOPO-II and PARP-1 was statistically significant. Analyses of DNA damage in BT-20 cells after 72 h showed that the 48 h post-incubation only increased tail intensity for cells treated with the topoisomerase II inhibitor at the lower dose. This puzzling result was explained by fluorescence microscopy studies, which revealed that following the initial treatment, the level of DNA damage increased during the 48 h post-incubation period. It should be noted that it is not possible to determine the intensity of the tail in cells in which nuclear DNA has been destroyed using the computer-aided Comet assay image analysis system (Comet Assay IV, Perceptive Instruments, UK); we have addressed this problem previously [37].

4. Discussion

Malfunctions in the control of cell proliferation can be more or less specifically countered using drugs that interfere with DNA replication, cell cycle progression, cell division and transcription. One possible way of achieving this is by using pharmacological agents that directly target DNA topoisomerases. Topoisomerases (of both type I and type II) play a key role in the control of DNA

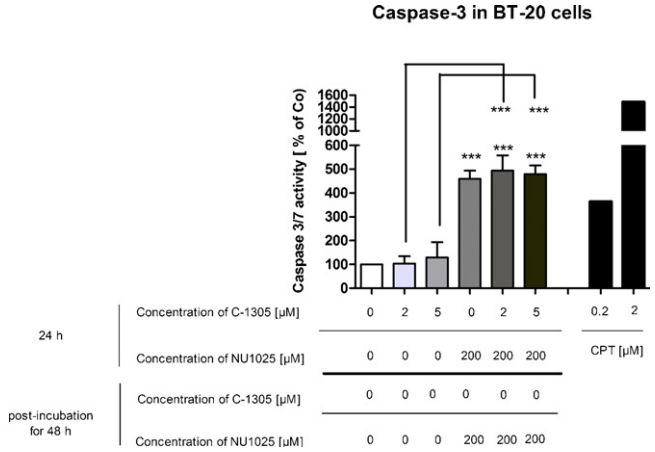

Fig. 9. Inactivation of PARP-1 strongly induces caspase-3 in BT-20 cells. Inhibition of PARP-1 strongly induces activity of caspase-3 in BT-20 cells. Exponentially growing BT-20 cells were treated in a multiwell plate with drugs at indicated concentrations. The activity of caspase-3 was determined in quadruplicate using the Caspase-3 GLO assay. The activity of the effector caspase [relative luminescence units (RLU)] was normalized to the numbers of viable cells, determined in parallel by CellTiter Glo assay. The data represent mean values ± SD from two independent experiments. The statistical significance of the activation of caspase-3 after treatment was calculated using Bonferroni's Multiple Comparison test. BT-20 cells exposed to CPT for 72 h were used as a positive control. Asterisks located directly above individual bars denote statistically significant differences between the corresponding treatment and the control. Asterisks located directly at the end of a line connecting two bars denote statistically significant differences between the indicated treatments. Triple asterisks denote significant differences at the $p < 0.001$ level.

topology [38,39]. Cellular processes such as DNA replication, transcription and recombination require that the relevant enzymes have physical access to the chromosomes' nucleotide bases [40]. Topoisomerases change the topology of nuclear DNA and can "unwind" it, thereby making the nucleotides accessible [41].

Topoisomerase expression is deregulated in many cancer cells [42]. Inhibiting topoisomerases activity removes the cell's ability to change the topology of its DNA and thus blocks DNA synthesis and sister chromatid segregation. These essential cellular functions of DNA topoisomerases make them excellent targets for anticancer drugs [10]. Several pharmacological topoisomerase inhibitors generate DNA strand breaks. If these breaks remain unrepaired, they accumulate, leading to apoptosis (for reviews, [10,42]).

There are two types of agents that target topoisomerases, both of which interfere with at least one step of the enzymes' catalytic cycle [10]. Notably, cancer cells carrying mutations in *BRCA1/2* exhibit increased sensitivity to topoisomerase inhibitors. The *BRCA1/2* tumor suppressor genes that are often mutated in breast and ovarian cancers [43] encode proteins involved in DNA repair processes, mainly in the HR [44–46]. As such, the loss of *BRCA1/2* or disruption of their activity reduces or even eliminates the cells' ability to properly repair damaged DNA and maintain genome stability [43,47].

In the study reported herein, we determined the anti-proliferative and pro-apoptotic effects of C-1305, a selective inhibitor of topoisomerase II on human breast cancer cell lines with different *BRCA1* and *p53* statuses. The lines responded differently to inhibition of topoisomerase II. BT-20 cells with strong expression of BRCA1 were resistant to C-1305 whereas MCF-7 cells and SKBr-3 cells were more sensitive. However,

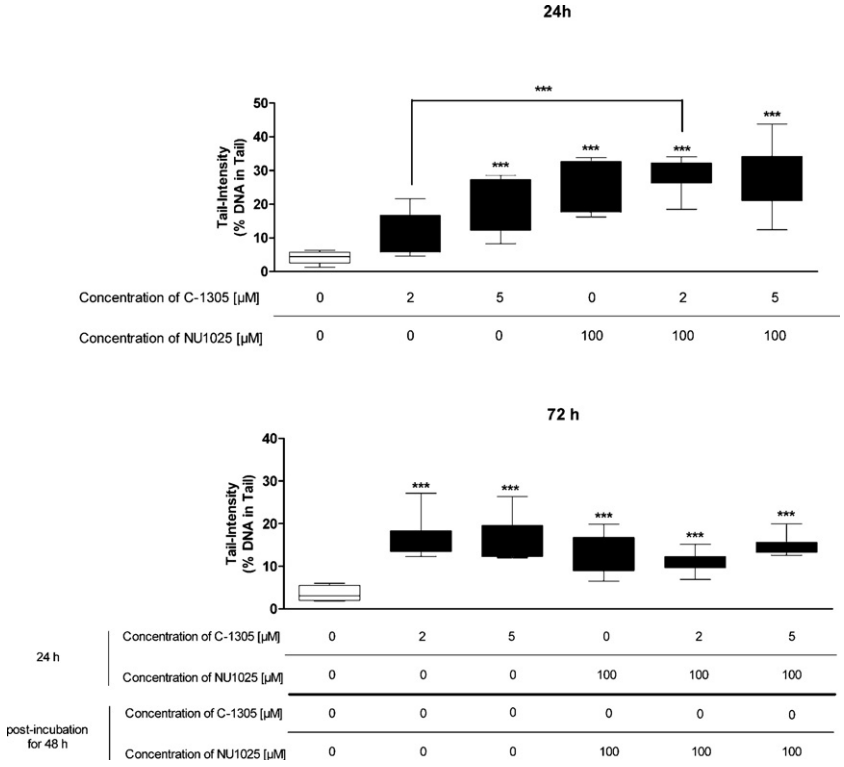

Fig. 10. Accumulation of DNA strand breaks in BT-20 cells after inhibition of PARP-1. Untreated human BT-20 cells and cells treated with C-1305, NU1025 or their combination at indicated concentrations were resolved by electrophoresis and the gels were stained with ethidium bromide (20 μg/ml). The resulting slides were examined under a fluorescence microscope (Nikon EFD-3, Tokyo, Japan) using 25-fold magnification. DNA migration was determined based on tail intensity (% DNA in tail) using a computer-aided Comet assay image analysis system (Comet Assay IV, Perceptive Instruments, UK). The statistical significance was determined using Dunnett's and Benferroni's Multiple Comparison test. Plots = mean ± SD of two independent experiments. Asterisks located directly above individual bars denote statistically significant differences between the corresponding treatment and the control. Asterisks located directly at the midpoint of a line connecting two bars denote statistically significant differences between the indicated treatments. Triple asterisks denote significant differences at the $p < 0.001$ level.

BRCA1-competent (MCF-7) and BRCA1-deficient (SKBr-3) cells were almost equally affected by the inhibition of topoisomerase II. Our previous studies have shown that the inactivation of PARP-1 in mouse and human cells greatly enhances the cytotoxic activity of triazoloacridone C-1305 [24,48]. We attributed this increased cytotoxicity of NU1025/C-1305 combination to a partial re-activation of wt p53 pathway in drug-treated HeLa cells and a more stringent cell cycle checkpoint control during G_2/M transition that was associated with the enhanced cell death by mitotic catastrophe [48]. These findings prompted us to determine whether pharmacological inhibition of PARP-1 might potentiate the cytotoxicity of C-1305 in breast cancer cells. It has previously been shown that *BRCA1/2* deficient cancer cells are extremely sensitive to pharmacological inhibition of PARP-1 [15,16]. Based on these data, one would expect that PARP-1 inhibition in BRCA-1 deficient SKBr-3 cells would be cytotoxic and would enhance the anti-proliferative effect of the topoisomerase II inhibitor. Surprisingly, this was not the case: pharmacological interference with PARP-1 had almost no effect on SKBr-3 proliferation and was not synergistic with the effects of C-1305. In contrast, the PARP-1 inhibitor NU1025 strongly inhibited the proliferation of BT-20 breast cancer cells that express high levels of BRCA1. The decrease in the number of viable BT-20 cells upon PARP-1 inhibition was associated with the strong accumulation of cells arrested at the G_2/M transition and concomitant induction of caspase-dependent apoptosis. Moreover, NU1025 potentiated the efficacy of C-1305 treatment. The interaction between both compounds was highly synergistic in almost all tested combinations. These unexpected findings raised question about the mechanisms of the increased cytotoxicity of C-1305 when applied in conjunction with the PARP-1 inhibitor. Further experiments revealed that the inhibition of PARP-1 in BT-20 cells resulted in the accumulation of DNA strand breaks and induced caspase-3 dependent apoptosis. These results seem to indicate that inhibiting PARP-1 can potentiate the cytotoxicity of anti-cancer drugs in cancer cells with functional BRCA1 and suggest that mutations in other DNA repair proteins may render cancer cells more sensitive to interference with PARP-1 activity.

The origin of the synergy between PARP-1 inhibition and C-1305 was not immediately apparent. A comparison of the site-specific phosphorylation of H2AX after inhibition of TOPO II in the studied breast cancer cells revealed that C-1305 induced phosphorylation of Ser139 in the H2AX protein in MCF-7 but not in BT-20 cells. In contrast, NU1025 alone induced phosphorylation of H2AX at Ser139 in BT-20 but not in MCF-7 cells; when NU1025 was applied in conjunction with C-1305, the abundance of this H2AX modification increased in both cancer cell lines. However, the increase in H2AX phosphorylation was much more pronounced in BT-20 cells. The two cell lines differ in terms of BRCA1 expression and also in terms of the functional status of *TP53*. MCF-7 cells express the active wt form of the p53 tumor suppressor whereas BT-20 cells express an inactive mutant form. Notably, TOPO II inhibition strongly induced p53 expression in MCF-7 cells in tandem with the increased H2AX phosphorylation. Cellular levels of the p53 protein also increased in MCF-7 cells in a concentration-dependent manner following treatment with NU1025. This indicates that DNA damage signaling was occurring in the MCF-7 cells, inducing a cellular response to the inhibition of the two enzymes whereas in BT-20 cells the response was primarily due to PARP-1 inhibition alone. PARP-1 is an abundant nuclear enzyme that exhibits near-ubiquitous expression and has multiple functions in the cell; it has been reported to be involved in DNA-damage-dependent remodeling of the chromatin, DNA repair, replication and recombination, cell cycle control, the transcription of the wt p53 protein and the regulation of its stability [49,50]. Studies on PARP-1 knock-out (KO) mice provided important evidence for the physiological roles of PARP-1. Overall, the results obtained using the KO mouse experimental model revealed that although PARP-1 is dispensable for life, development and differentiation, life in the absence of PARP-1 is associated with increased genomic instability because it reduces the cell's ability to detect and repair DNA lesions. The strong sensitivity of BT-20 cells to PARP-1 inhibition and the associated accumulation of DNA strand breaks seems to be indicative of a DNA repair deficiency in this line.

Damage to cellular genetic material is an ongoing threat to both a cell's ability to maintain genetic stability and to the error-free transmission of genetic information to daughter cells. DNA can be damaged spontaneously during DNA metabolism or normal cellular metabolism. Breaks in DNA strands can be generated by the free radicals (*e.g.* oxygen radicals and other reactive oxygen species) that are formed as products of cellular respiration [51]. Moreover, environmental damage to DNA can be caused by exogenous chemical or physical factors [52]. In the context of the results collected in this study, it should be noted that numerous drugs (including topoisomerase inhibitors) cause severe damage to DNA in both cancerous and healthy cells. Serendipitously, while DNA can be damaged in various ways, it is also amenable to repair. Indeed, cells have various means of repairing DNA, which are important if the accumulation of DNA damage and the resulting genomic instability are to be avoided. The cellular response to DNA damage signaling is dependent on the type of lesions present and involves the activation of factors involved in the appropriate repair pathways. Base-excision repair (BER), nucleotide-excision repair (NER) and mismatch-repair (MM) are essential for the elimination of single-strand breaks (SSB), whereas HR [53,54] and NHEJ [55,56] serve to repair double strand breaks (DSBs). The DNA damage signaling and repair pathways are regulated by a number of cellular proteins. The functional status of these proteins and the smoothness of their coordination determine the efficacy of DNA repair. PARP-1, a nuclear enzyme, is a very sensitive detector of DNA breaks [57,58]. Remarkably, there are several points of overlap and redundancies in the various signaling and repair pathways.

These overlaps are illustrated by the case of breast and ovarian cancer type 1 susceptibility protein (BRCA1), which is a tumor suppressor [8]. BRCA1 is a large protein that contains an amino-terminal RING domain and is a crucial component of the HR-mediated repair of DSBs [59,60]. However, it can also participate in other DNA repair pathways such as NER [45], NHEJ [44] and transcription-coupled repair [61]. BRCA1 is expressed during the S- and G_2-phases of the cell cycle and forms stable complexes with BRCA1-associated RING domain protein 1 (BARD1) *via* its RING domain [62]. BRCA1, a phosphoprotein, harbors at least 14 serine residues that can be modified by several protein kinases (reviewed in [63]). At least seven potential residues fitting ATM's modification motif (S/T-Q) are phosphorylated by ATM kinase *in vitro* and *in vivo*. DNA damage triggers ATM/ATR-dependent phosphorylation of histone H2AX at Ser139 (H2AX phosphorylated in this way is known as γ-H2AX) [64]. Subsequently, γ-H2AX recruits mediator of DNA damage checkpoint 1 (MDC1), which in turn mediates the accumulation of the E3 ligase RNF8 complex to promote ubiquitylation of histones and other proteins at the sites of DNA breaks and optionally RNF168 [65]. In response to DNA injury, BRCA1 is rapidly phosphorylated, prompting its relocation to damage-induced foci whose position is marked by the γ-H2AX) [64]. At these foci, BRCA1 is recruited by RAP80 and co-localizes with the DNA repair protein RAD51 [66], the meiotic recombination 11 (MRE11)-RAD50-NBS1 (nibrin) protein (MRN complex) and several other proteins involved in DNA damage signaling and repair such as ABRAXAS, BRCA2, CtBP-interacting protein (CtIP), Receptor-Associated Protein 80 (RAP80), Mediator of Rap80

Interactions and Targeting 40 kDa (MERIT40), and Partner And Localizer of BRCA2 (PALB2 also known as FANCN). This process generates multiple macro-complexes (for a review, see [8]). This raises a question: how does BRCA1 regulate DNA repair? It seems to play at least two roles at damage-induced foci. First, it acts as a scaffolding factor that facilitates ATM/ATR-mediated signaling (which in turn affects the activity of proteins such as p53, nibrin, Chk1 and Chk2). Second, it recruits specific proteins involved in the regulation of DNA repair and coordinates their assembly [8]. To facilitate HR-mediated repair, DSBs need to be processed to generate ssDNA sections. These then allow the recruitment of the RAD51 protein. There is evidence suggesting that BRCA1 might also participate in DNA end resection, thereby facilitating the formation of RAD51 nucleoprotein filaments [8]. The finding discussed above indicate that the BRCA1 protein has important function in the maintenance of genome integrity *via* processes of DNA replication and repair, especially in the error-free repair of DSBs by HR [8]. In the absence of BRCA1, HR is impaired and DSBs have to be processed using alternative mechanisms such as the error-prone NHEJ. However, considering the complexity of the DNA repair pathways, it is conceivable that deficits in other proteins involved in HR or components of the DNA damage signaling machinery could also severely hinder the repair of damaged DNA.

Deficit(s) in DNA repair provided a rationale for the development of synthetic lethality, a new therapeutic strategy. According to the concept of synthetic lethality, dysfunctions in either of the DNA repair genes alone would be compatible with cell viability but simultaneous mutation (inactivation) of both would cause cell death. Our results clearly indicate that pharmacological inhibition of PARP-1 is conditionally synthetic lethal in BT-20 but not in MCF-7 or SKBr-3 breast cancer cells. These observations are consistent with recent reports indicating that synthetic lethality can be achieved in cancer cells carrying mutations in other DNA repair genes. Thus, cells carrying bi-allelic mutations in the *phosphatase tensin homolog* (PTEN) display defects in HR and are sensitive to PARP-1 inhibition [67,68] Furthermore, ATM-deficient mantle cell lymphoma cells (MTL) that are defective in DNA damage signaling and cell cycle checkpoint control are more sensitive to PARP-1 inhibitors than the ATM-proficient MCF cells [69].

The selectivity of PARP inhibitors toward cancer cells, together with their suitability for use in tandem with other drugs and in multimodal therapies make them promising agents for use clinical oncology.

Acknowledgments

We thank Dr. I. Herbacek for performing the flow cytometric measurements and Mr. P. Breit for preparation of images from fluorescence microscopy.

References

[1] DeSantis C, Siegel R, Bandi P, Jemal A. Breast cancer statistics, 2011. CA Cancer J Clin 2011;61:409–18.
[2] Siegel R, Naishadham D, Jemal A. Cancer statistics, 2012. CA Cancer J Clin 2012;62:10–29.
[3] Bertos NR, Park M. Breast cancer – one term, many entities. J Clin Invest 2011; 121:3789–96.
[4] Russnes HG, Navin N, Hicks J, Borresen-Dale AL. Insight into the heterogeneity of breast cancer through next-generation sequencing. J Clin Invest 2011; 121:3810–8.
[5] Higgins MJ, Baselga J. Targeted therapies for breast cancer. J Clin Invest 2011; 121:3797–803.
[6] Greene MH. Genetics of breast cancer. Mayo Clin Proc 1997;72:54–65.
[7] Miki Y, Swensen J, Shattuck-Eidens D, Futreal PA, Harshman K, Tavtigian S, et al. A strong candidate for the breast and ovarian cancer susceptibility gene BRCA1. Science 1994;266:66–71.
[8] Huen MS, Sy SM, Chen J. BRCA1 and its toolbox for the maintenance of genome integrity. Nat Rev Mol Cell Biol 2010;11:138–48.
[9] Roy R, Chun J, Powell SN. BRCA1 and BRCA2: important differences with common interests. Nat Rev Cancer 2012;12:372.
[10] Wesierska-Gadek J, Skladanowski A. Therapeutic intervention by the simultaneous inhibition of DNA repair and type I or type II DNA topoisomerases: one strategy, many outcomes. Future Med Chem 2012;4:51–72.
[11] Binaschi M, Zunino F, Capranico G. Mechanism of action of DNA topoisomerase inhibitors. Stem Cells 1995;13:369–79.
[12] Vogel EW, Barbin A, Nivard MJ, Stack HF, Waters MD, Lohman PH. Heritable and cancer risks of exposures to anticancer drugs: inter-species comparisons of covalent deoxyribonucleic acid-binding agents. Mutat Res 1998;400: 509–40.
[13] Royle JA, Baade PD, Joske D, Girschik J, Fritschi L. Second cancer incidence and cancer mortality among chronic lymphocytic leukaemia patients: a population-based study. Br J Cancer 2011;105:1076–81.
[14] Fulda S. Targeting apoptosis signaling pathways for anticancer therapy. Front Oncol 2011;1–7.
[15] Bryant HE, Schultz N, Thomas HD, Parker KM, Flower D, Lopez E, et al. Specific killing of BRCA2-deficient tumours with inhibitors of poly(ADP-ribose) polymerase. Nature 2005;434:913–7.
[16] Farmer H, McCabe N, Lord CJ, Tutt AN, Johnson DA, Richardson TB, et al. Targeting the DNA repair defect in BRCA mutant cells as a therapeutic strategy. Nature 2005;434:917–21.
[17] Hay T, Matthews JR, Pietzka L, Lau A, Cranston A, Nygren AO, et al. Poly(ADP-ribose) polymerase-1 inhibitor treatment regresses autochthonous Brca2/p53-mutant mammary tumors in vivo and delays tumor relapse in combination with carboplatin. Cancer Res 2009;69:3850–5.
[18] Hay T, Jenkins H, Sansom OJ, Martin NM, Smith GC, Clarke AR. Efficient deletion of normal Brca2-deficient intestinal epithelium by poly(ADP-ribose) polymerase inhibition models potential prophylactic therapy. Cancer Res 2005;65:10145–48.
[19] McCabe N, Lord CJ, Tutt AN, Martin NM, Smith GC, Ashworth A. BRCA2-deficient CAPAN-1 cells are extremely sensitive to the inhibition of poly (ADP-Ribose) polymerase: an issue of potency. Cancer Biol Ther 2005;4:934–6.
[20] Kaelin Jr WG. The concept of synthetic lethality in the context of anticancer therapy. Nat Rev Cancer 2005;5:689–98.
[21] Lasfargues EY, Ozzello L. Cultivation of human breast carcinomas. J Natl Cancer Inst 1958;21:1131–47.
[22] Thompson C, MacDonald G, Mueller CR. Decreased expression of BRCA1 in SK-BR-3 cells is the result of aberrant activation of the GABP Beta promoter by an NRF-1-containing complex. Mol Cancer 2011;10:62.
[23] Wesierska-Gadek J, Gueorguieva M, Horky M. Roscovitine-induced up-regulation of p53AIP1 protein precedes the onset of apoptosis in human MCF-7 breast cancer cells. Mol Cancer Ther 2005;4:113–24.
[24] Wesierska-Gadek J, Schloffer D, Gueorguieva M, Uhl M, Skladanowski A. Increased susceptibility of poly(ADP-ribose) polymerase-1 knockout cells to antitumor triazoloacridone C-1305 is associated with permanent G2 cell cycle arrest. Cancer Res 2004;64:4487–97.
[25] Wesierska-Gadek J, Gueorguieva M, Ranftler C, Zerza-Schnitzhofer G. A new multiplex assay allowing simultaneous detection of the inhibition of cell proliferation and induction of cell death. J Cell Biochem 2005;96:1–7.
[26] Kovar H, Jug G, Printz D, Bartl S, Schmid G, Wesierska-Gadek J. Characterization of distinct consecutive phases in non-genotoxic p53-induced apoptosis of Ewing tumor cells and the rate-limiting role of caspase 8. Oncogene 2000; 19:4096–107.
[27] Wesierska-Gadek J, Schmid G. Overexpressed poly(ADP-ribose) polymerase delays the release of rat cells from p53-mediated G(1) checkpoint. J Cell Biochem 2000;80:85–103.
[28] Vindelov LL. Flow microfluorometric analysis of nuclear DNA in cells from solid tumors and cell suspensions. A new method for rapid isolation and straining of nuclei. Virchows Arch B Cell Pathol 1977;24:227–42.
[29] Tice RR, Agurell E, Anderson D, Burlinson B, Hartmann A, Kobayashi H, et al. Single cell gel/comet assay: guidelines for in vitro and in vivo genetic toxicology testing. Environ Mol Mutagen 2000;35:206–21.
[30] Hartmann A, Agurell E, Beevers C, Brendler-Schwaab S, Burlinson B, Clay P, et al. Recommendations for conducting the in vivo alkaline Comet assay.In: 4th international comet assay workshop. Mutagenesis 2003;18:45–51.
[31] Lindl T, Bauer J. Zell- und Gewebekultur: Einführung in die Grundlagen sowie ausgewählte Methoden und Anwendungen. Stuttgart/Jena/New York: Gustav Fischer; 1994. p. 94.
[32] Wesierska-Gadek J, Schloffer D, Kotala V, Horky M. Escape of p53 protein from E6-mediated degradation in HeLa cells after cisplatin therapy. Int J Cancer 2002;101:128–36.
[33] Wesierska-Gadek J, Bohrn E, Herceg Z, Wang ZQ, Wurzer G. Differential susceptibility of normal and PARP knock-out mouse fibroblasts to proteasome inhibitors. J Cell Biochem 2000;78:681–96.
[34] Chou TC, Talalay P. Quantitative analysis of dose-effect relationships: the combined effects of multiple drugs or enzyme inhibitors. Adv Enzyme Regul 1984;22:27–55.
[35] Reers M, Smith TW, Chen LB. J-aggregate formation of a carbocyanine as a quantitative fluorescent indicator of membrane potential. Biochemistry 1991;30:4480–6.
[36] Gottlieb E, Armour SM, Harris MH, Thompson CB. Mitochondrial membrane potential regulates matrix configuration and cytochrome c release during apoptosis. Cell Death Differ 2003;10:709–17.

[37] Wesierska-Gadek J, Gueorguieva M, Komina O, Schmid G, Kramer MP. Signaling of DNA damage is not sufficient to induce p53 response: (re)activation of wt p53 protein strongly depends on cellular context. J Cell Biochem 2008; 103:1607–20.
[38] Champoux JJ. DNA topoisomerases: structure, function, and mechanism. Annu Rev Biochem 2001;70:369–413.
[39] Wang JC. Moving one DNA double helix through another by a type II DNA topoisomerase: the story of a simple molecular machine. Q Rev Biophys 1998;31:107–44.
[40] Sundin O, Varshavsky A. Arrest of segregation leads to accumulation of highly intertwined catenated dimers: dissection of the final stages of SV40 DNA replication. Cell 1981;25:659–69.
[41] Schoeffler AJ, Berger JM. DNA topoisomerases: harnessing and constraining energy to govern chromosome topology. Q Rev Biophys 2008;41:41–101.
[42] Nitiss JL. Targeting DNA topoisomerase II in cancer chemotherapy. Nat Rev Cancer 2009;9:338–50.
[43] Antoniou A, Pharoah PD, Narod S, Risch HA, Eyfjord JE, Hopper JL, et al. Average risks of breast and ovarian cancer associated with BRCA1 or BRCA2 mutations detected in case Series unselected for family history: a combined analysis of 22 studies. Am J Hum Genet 2003;72:1117–30.
[44] Bau DT, Mau YC, Shen CY. The role of BRCA1 in non-homologous end-joining. Cancer Lett 2006;240:1–8.
[45] Hartman AR, Ford JM. BRCA1 induces DNA damage recognition factors and enhances nucleotide excision repair. Nat Genet 2002;32:180–4.
[46] Snouwaert JN, Gowen LC, Latour AM, Mohn AR, Xiao A, DiBiase L, et al. BRCA1 deficient embryonic stem cells display a decreased homologous recombination frequency and an increased frequency of non-homologous recombination that is corrected by expression of a brca1 transgene. Oncogene 1999;18: 7900–7.
[47] Pellegrini L, Venkitaraman A. Emerging functions of BRCA2 in DNA recombination. Trends Biochem Sci 2004;29:310–6.
[48] Sabisz M, Wesierska-Gadek J, Skladanowski A. Increased cytotoxicity of an unusual DNA topoisomerase II inhibitor compound C-1305 toward HeLa cells with downregulated PARP-1 activity results from re-activation of the p53 pathway and modulation of mitotic checkpoints. Biochem Pharmacol 2010;79:1387–97.
[49] Wesierska-Gadek J, Wang ZQ, Schmid G. Reduced stability of regularly spliced but not alternatively spliced p53 protein in PARP-deficient mouse fibroblasts. Cancer Res 1999;59:28–34.
[50] Wesierska-Gadek J, Wojciechowski J, Schmid G. Phosphorylation regulates the interaction and complex formation between wt p53 protein and PARP-1. J Cell Biochem 2003;89:1260–84.
[51] Lonkar P, Dedon PC. Reactive species and DNA damage in chronic inflammation: reconciling chemical mechanisms and biological fates. Int J Cancer 2011; 128:1999–2009.
[52] Hoeijmakers JH. DNA damage, aging, and cancer. N Engl J Med 2009; 361:1475–85.
[53] Khanna KK, Jackson SP. DNA double-strand breaks: signaling, repair and the cancer connection. Nat Genet 2001;27:247–54.
[54] Heyer WD, Ehmsen KT, Liu J. Regulation of homologous recombination in eukaryotes. Annu Rev Genet 2010;44:113–39.
[55] van Gent DC, Hoeijmakers JH, Kanaar R. Chromosomal stability and the DNA double-stranded break connection. Nat Rev Genet 2001;2:196–206.
[56] Lieber MR. The mechanism of double-strand DNA break repair by the nonhomologous DNA end-joining pathway. Annu Rev Biochem 2010;79:181–211.
[57] Schreiber V, Dantzer F, Ame JC, de Murcia G. Poly(ADP-ribose): novel functions for an old molecule. Nat Rev Mol Cell Biol 2006;7:517–28.
[58] Luo X, Kraus WL. On PAR with PARP: cellular stress signaling through poly(-ADP-ribose) and PARP-1. Genes Dev 2012;26:417–32.
[59] Moynahan ME, Chiu JW, Koller BH, Jasin M. Brca1 controls homology-directed DNA repair. Mol Cell 1999;4:511–8.
[60] Moynahan ME, Cui TY, Jasin M. Homology-directed DNA repair, mitomycin-c resistance, and chromosome stability is restored with correction of a Brca1 mutation. Cancer Res 2001;61:4842–50.
[61] Abbott DW, Thompson ME, Robinson-Benion C, Tomlinson G, Jensen RA, Holt JT. BRCA1 expression restores radiation resistance in BRCA1-defective cancer cells through enhancement of transcription-coupled DNA repair. J Biol Chem 1999;274:18808–12.
[62] Meza JE, Brzovic PS, King MC, Klevit RE. Mapping the functional domains of BRCA1. Interaction of the ring finger domains of BRCA1 and BARD1. J Biol Chem 1999;274:5659–65.
[63] Ouchi T. BRCA1 phosphorylation: biological consequences. Cancer Biol Ther 2006;5:470–5.
[64] Rogakou EP, Pilch DR, Orr AH, Ivanova VS, Bonner WM. DNA double-stranded breaks induce histone H2AX phosphorylation on serine 139. J Biol Chem 1998;273:5858–68.
[65] Doil C, Mailand N, Bekker-Jensen S, Menard P, Larsen DH, Pepperkok R, et al. RNF168 binds and amplifies ubiquitin conjugates on damaged chromosomes to allow accumulation of repair proteins. Cell 2009;136:435–46.
[66] Scully R, Chen J, Plug A, Xiao Y, Weaver D, Feunteun J, et al. Association of BRCA1 with Rad51 in mitotic and meiotic cells. Cell 1997;88:265–75.
[67] Mendes-Pereira AM, Martin SA, Brough R, McCarthy A, Taylor JR, Kim JS, et al. Synthetic lethal targeting of PTEN mutant cells with PARP inhibitors. EMBO Mol Med 2009;1:315–22.
[68] Williamson CT, Muzik H, Turhan AG, Zamo A, O'Connor MJ, Bebb DG, et al. ATM deficiency sensitizes mantle cell lymphoma cells to poly(ADP-ribose) polymerase-1 inhibitors. Mol Cancer Ther 2010;9:347–57.
[69] Ding L, Getz G, Wheeler DA, Mardis ER, McLellan MD, Cibulskis K, et al. Somatic mutations affect key pathways in lung adenocarcinoma. Nature 2008;455: 1069–75.